JOURNAL OF GEOPHYSICAL RESEARCH, VOL. 87, NO. C12, PAGES 9499–9508, NOVEMBER 20, 1982

Energy Saturation and Phase Speeds Measured on a Natural Beach

EDWARD B. THORNTON

Naval Postgraduate School, Monterey, California 93940

R. T. GUZA

Shore Processes Laboratory, Scripps Institution of Oceanography, University of California, La Jolla, California 92037

Field measurements of wave height and speed from 7-m depth shoreward are described. The experiment plan consisted of a shore-normal transect of closely spaced (compared to a dominant wave length) velocity, pressure, and elevation sensors on an almost plane profile having an inshore slope of 1:50. As the waves shoal and begin to break, the dominant dissipative mechanism is due to turbulence generated at the crest, and wave heights become increasingly depth controlled as they progress across the surf zone. Wave heights in the inner surf zone are strongly depth dependent; the envelope of the wave heights is described by $H_{rms} = 0.42$ h. The depth dependence of the breaking wave height is shown to be related to the kinematic instability criterion. Celerity spectra were measured by using phase spectra calculated between pairs of adjacent sensors. Inshore of 4-m depth, the celerity was found distant over the energetic region of the spectrum. A 'mean' celerity was compared with linear theory and was within +20% and −10%, showing good agreement for such a nonlinear, dissipative region.

INTRODUCTION

Two basic variables requiring description in the various modern theories of wave-induced longshore currents [*Bowen*, 1969; *Longuet-Higgins*, 1970; *Thornton*, 1971] are the wave height (H) inside the surf zone and the wave speed (C) in shallow water. These two parameters together with the local depth (h) are used to specify (to first order) the amplitude of the horizontal shallow water velocities

$$|u|, |v| = \frac{H}{2}\frac{g}{C}(\cos\alpha, \sin\alpha) \quad (1)$$

where α is the local angle of wave incidence with the normal to the bottom contour. The local angle of wave incidence on plane beaches is related to a reference wave angle, either in deep water or at breaking, using Snell's law of wave refraction, which itself contains the wave speed. The horizontal velocities are used to describe the off-axis wave-induced momentum flux (i.e., radiation stress). The radiation stress is the primary driving force for longshore currents, and its specification forms the basis for the various theories.

It is assumed in the above theories that the wave heights at breaking and inside the surf zone are linearly dependent on depth, $H = \gamma h$, simulating spilling breakers gradually losing energy across the surf zone. The proportionality factor, γ, in the above models was taken either as 0.78 corresponding to breaking conditions for a solitary wave or values ranging between 0.8 and 1.2 corresponding to laboratory experiments by *Galvin and Eagleson* [1965]. The great simplification of assuming wave height proportional to depth is that the energy is described everywhere without having to worry about how the dissipative processes of breaking waves occur.

The phase speed in the theories is described by using either linear theory or solitary theory. The use of the solitary wave breaking criteria and phase speed is based on solitary wave theory giving a qualitative description of the shallow water wave profile while retaining nonlinear effects (i.e., amplitude dispersion).

This paper examines the shoaling and subsequent breaking of waves measured from 7-m depth shoreward on a gently sloping ($\beta \sim 0.02$) fine grained sandy beach. The waves broke as spilling or mixed spilling-plunging. Surface elevation and horizontal, orthogonal velocity components were measured by using a closely spaced array in a shore-normal transect from offshore at the 7-m depth contour to across the surf zone (see Figure 6 in *Thornton and Guza* [1982], henceforth referenced to as TG82). A primary difference between these and past field experiments is the relatively close spacing of measurement locations (compared to the wave length of the dominant wave period) along a transect on a relatively simple, almost plane beach profile.

The transformation of the wave height and phase speed are described and compared with the field measurements. In the first section, wave height changes from offshore and at breaking and inside the surf zone are described. It is found that the waves are 'energy saturated' in the inner surf zone region demonstrated by a strong wave height dependence on depth. Celerity, or wave speed, measurements are described in the second section. Inside the 5-m depth contour, the measurements suggest the waves are frequency nondispersive but can be weakly amplitude dispersive.

EXPERIMENT

Field measurements were made at Torrey Pines Beach near San Diego, California, during November 1978. The beach and nearshore is gently sloping with nearly parallel and plane contours. The bottom is composed of moderately sorted, fine-grain sand (mean diameter 0.15–0.2 mm). A wide variety of wave and weather conditions were encountered during the experiment, from small to large (2 m) waves, from very narrow-band swell to wind-band sea, from calm to windy days (>10 m/s).

The instruments used in this study included a total of four

Paper number 2C1224.

TABLE 1. Location and Depth of Instruments (November 17)

	Distance Offshore Rel. Benchmark (m)	Depth Rel. msl (cm)	Δs, Dist. Between Inst. (m)
P7	442	−722	
			57
P7A	385	−659	
			69
C9	316	−547	
			75
C15	241	−325	
			30
C19	211	−220	
			26
C22, W29	185	−152	
			15
C23	170	−142	
			15
C31, W21, P30	155	−139	
			12
C36	143	−104	
			14
C37, W38	129	−77	
			14
C39	115	−51	
			16
C40, W29	99	−27	
			14
C42	85	+10	

wave staffs, a pressure sensor, and 11 electromagnetic current meters, arranged in a shore normal transect from 7-m depth to the shoreline. The offshore location, depth relative to mean sea level and distance between instruments used are given in Table 1. The experiments were normally conducted over the high tide so that the sea level during the experiment was usually about 1 m above msl.

The current meters are Marsh-McBirney 4-cm diameter electromagnetic flow meters which were oriented to measure horizontal orthogonal velocity components of x, onshore, and y, alongshore. The current meters and their calibration are described by *Cunningham et al.* [1979], who estimate their gain accuracy at ±5%.

The pressure sensors are Stathem temperature-compensated transducers with an accuracy of ±2% based on comparing precalibration and postcalibration gains. The wave staffs are dual resistance wires described in detail by *Flick et al.* [1979]; gain accuracy is about ±3%.

Data were telemetered to shore where they were simultaneously digitally recorded at a rate of 64 samples/s with synchronization errors less than 0.01 s. All data were digitally low passed with a 26 weight inverse transform filter, cut-off at 1.0 Hz. The data were then decimated to 2 samples/s, resulting in a Nyquist frequency of 1.0 Hz and minimal aliasing. Further details of the instrumentation, calibration, and installation is given in *Guza and Thornton* [1980] and TG82.

Wave Height Inside the Surf Zone

It has long been recognized that breaking wave height depends on the local depth. *McCowan* [1891], using solitary wave theory, found that the breaker height in shallow water is proportional to the depth at breaking, h_b

$$H_b = 0.78\, h_b \tag{2}$$

A further dependence on wave length L, or period, was shown theoretically by *Miche* [1954], where

$$H_b = 0.142\, L_b \tanh\left(\frac{2\pi h_b}{L_b}\right) \tag{3a}$$

which for shallow water reduces to the simple depth relationship

$$H_b = 0.89\, h_b \tag{3b}$$

Iversen [1952] performed experiments in the laboratory with beaches having steepnesses of 1/10, 1/20, and 1/50. He demonstrated a dependence of breaker height on beach slope with the breaker height to depth ratio increasing for steeper beaches. *Goda* [1970], and more recently *Weggel* [1972], synthesized a number of laboratory studies. *Weggel* [1972] empirically derived the breaker height as a function of local depth h_b, slope s, and period T, given by

$$\frac{H_b}{h_b} = b - \frac{aH_b}{gT^2} \tag{4}$$

where

$$a = 43.75\,(1 - e^{-19s})$$

$$b = \frac{1.56}{(1 + e^{-19.5s})}$$

The depth dependence of the observed rms wave height can be seen in Figure 1; 34 min averages of H_{rms} were estimated from the surface elevation variance, m_0, calculated from the horizontal velocity spectra applying a linear theory spectral transfer function, $H(f)$, and integrating across the spectra

$$H_{rms} = \sqrt{8m_0}$$

$$= 2\sqrt{2}\left\{\int_{0.05}^{0.67} |H(f)|^2[G_u^m(f) + G_v^m(f)]df\right\}^{1/2} \tag{5}$$

where $G_u^m(f)$ and $G_v^m(f)$ are the measured (x, y) horizontal velocity spectra. The use of linear transfer functions is justified by intercomparisons of elevation and velocity spectra [*Guza and Thornton*, 1980]. Since the measurements are in very shallow water, a significant portion of the spectral energy can be contained in the low frequencies due to surf beat and edge waves which do not break and are not depth limited due to saturation. To eliminate low frequency contamination, the spectra in (5) are integrated only over the seaswell band of frequencies from .05 to 0.67 Hz. The

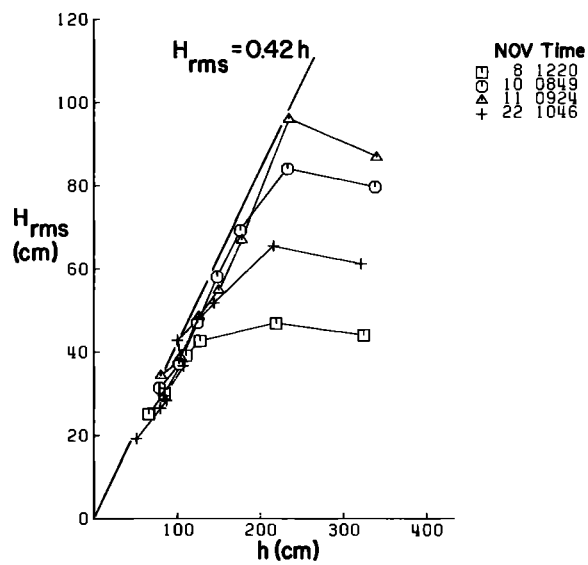

Fig. 1. H_{rms} inferred from velocity using (15) versus depth demonstrating wave height in the inner surf zone is locally depth controlled.

calculated rms wave height, H_{rms}, is approximately proportional to $\sqrt{m_0}$ for random waves, exactly for a linear process with sinusoidal waves [*Longuet-Higgins*, 1980], but was shown for this same data by TG82 to be a good approximation with an average error of only −0.3%. The comparison depths were calculated by using the nearest wave staff or pressure sensor. Set-up is taken into account by using direct measures of the depth. Starting from offshore and following a particular curve, the wave height initially increases and then curves over until in shallow water all waves tend to decay in approximately the same manner. The waves plotted in Figure 1 demonstrate the wind-wave height in the inner surf zone is essentially independent of the wave height outside the surf zone. Waves of the inner surf zone region are locally depth controlled and can be described as 'saturated periodic bores.'

The temporal variability of wave height calculated using (5) for 17.1 min averages is shown in Figure 2. Offshore (C15) and about the breakerline (C22), H_{rms} shows considerable temporal variability due to the statistical variability of the incoming wave variance. The furthest offshore location is C15 with onshore stations increasing in number. The variability of H_{rms} decreases inside the surf zone as the waves are no longer governed by outside conditions, but become locally depth controlled. The four most inshore measurement locations form quasi-parallel lines. The slow decreasing trend in H_{rms} of the waves inside the surf zone, while the heights of the waves outside do not show a decreasing trend, is due to the mean depth of the water decreasing during ebb tide, again emphasizing the depth dependence of wave height inside the surf zone. A random wave model that predicts inner surf zone saturation is given in TG82.

H_{rms} calculated by using velocity sensors are plotted against mean depth for all days in Figure 3. The mean position of the breakerline changed considerably over a tidal cycle so several data sets are presented for the same day. An approximate envelope for wave heights in the inner surf zone suggests a linear relationship

$$H_{rms} \simeq 0.42\ h \tag{6}$$

The envelope curve (6) represents a maximum H_{rms} relationship with depth.

No bottom slope dependence of H_{rms} can be ascertained from the measurements because the bottom slope was essentially the same on all days. The strong depth dependence in the inner surf zone is because a high proportion of

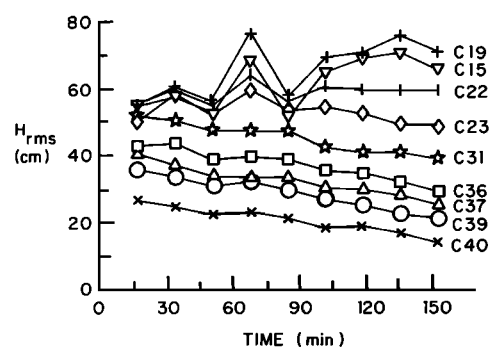

Fig. 2. H_{rms} inferred from velocity using (15) as a function of time demonstrating depth dependence of variance in inner surf zone, November 10, 1978. Current meter number is indicated.

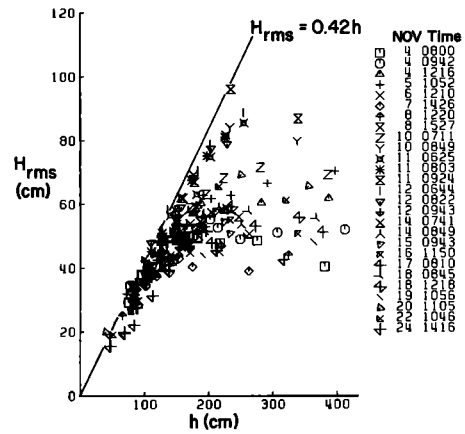

Fig. 3. H_{rms} inferred from velocity using (15) versus depth for all days.

waves are breaking (TG82). Wave heights in the outer surf zone region and about the average breakerline, where only some of the waves have broken (i.e., unsaturated) are not represented by a simple depth dependent relationship such as in (6). Therefore, the strong, quasi-linear depth dependence by the wave heights of the inner surf zone separates the region from the outer surf zone.

H_{rms} values calculated directly from the surface elevation variance measurements by using wave staffs are plotted against mean depth in Figure 4. There were at most five wave staffs on any single day located primarily inside the surf zone, so there are many fewer measurement points than for the current meter calculations. H_{rms} values calculated using current meters and measured using wave staffs result in essentially the same relationship with depth in the inner surf zone.

The strong dependence of H_{rms} on depth in the inner surf zone may be related to a kinematic instability criterion which asserts [*Banner and Phillips*, 1974] that breaking occurs when the horizontal velocity at the crest, u_c, exceeds the wave speed

$$u_c \geq C \tag{7}$$

Given that $H_{rms} = 0.42\ h$ (6), and using velocity measurements in the fluid interior with linear transfer functions, it follows that a direct calculation of wind wave crest rms velocity in shallow water yields

$$u_{rms}^{crest} = \frac{H_{rms}}{2}(g/h)^{1/2} = 0.21(gh)^{1/2} \tag{8}$$

the phase speed results presented below, however, show that $C \approx (gh)^{1/2}$ so that (8) is equivalent to

$$u_{rms}^{crest} \cong 0.21\ C \tag{9}$$

where both u and C are measured quantities. The kinematic instability criterion (7) is to be applied at the crest, however, while the velocity measurements are taken in the interior. Laboratory experiments [*Van Dorn*, 1976] with monochromatic waves on gentle slopes, show that crest particle velocities commonly exceed those in the interior by a factor of 5. Whether a similar proportionality holds in the field is not known; a factor of ~5 would imply that $u_{rms}^{crest} \simeq C$. *Hedges and Kirkgoz* [1981] found in laboratory studies $u_{crest} = C$ only applied to relatively mild slopes for

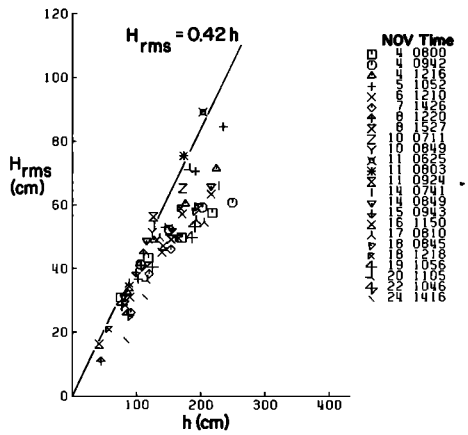

Fig. 4. H_{rms} calculated using surface elevation spectra versus depth for all days.

the case of spilling breakers. The main point is that a saturated wave height proportional to h is qualitatively consistent with breaking as expressed by the kinematic instability criterion (7). Spilling breakers on flat sloping beaches are most likely to behave in this way, as evidenced by the continuous breaking across the surf zone. Plunging breakers behave qualitatively differently in that they break more violently with rebounding waves from the plunge, and generate larger vortices that penetrate to a greater depth [*Miller*, 1976]. The broken wave, having given up considerable excess energy, reforms and progresses as an unbroken wave until it again meets the kinematic instability criterion.

CELERITY

Wave phase speed (celerity) of individual waves has been measured in a number of recent studies, both in the laboratory and field. *Svendsen et al.* [1978] and *Hedges and Kirkgoz* [1981] measured individual waves in laboratory studies of monochromatic breaking waves on various plane beaches (slopes 0.02–0.08) and found better agreement with bore theory than linear wave theory. *Suhayda and Pettigrew* [1977] measured the phase speed of 10 individual plunging waves across the surf zone in the field. They found the measured celerities were less than predicted by inviscid bore theory, except in a small area just shoreward of the break point. They concluded that turbulent dissipation had to be included in theory in order to describe quantitatively the wave height and celerity across the surf zone. *Inman et al.* [1971] measured the speed of individual spilling waves at Torrey Pines Beach, and found the phase speeds slightly greater than the linear prediction of $(\sqrt{gh})$ and less than the theoretical value for a solitary wave.

The measurement of phase speed by observing individual waves is only applicable in a nondispersive (or very weakly dispersive) system, or with monochromatic waves. *Ramamonjiarisoa et al.* [1978], and *Mitsuyasu et al.* [1979], made laboratory measurements of the celerity spectra of deep water wind-generated waves. Calculation of the phase difference between sensors, as a function of frequency, allows calculation of the phase speed as a function of frequency (i.e., the celerity spectrum). Both observed that wave celerities were the same at high frequencies (where linear theory indicated the celerity should decrease) as at the peak of the spectrum. They interpreted this as being due to nonlinear cross-spectral coupling.

Thornton et al. [1976], similarly inferred the wave celerity from the measured phase spectrum in the field between two closely spaced measurement locations just outside and within the surf zone. The celerity was again found constant over the energetic region of the spectrum. *Büsching* [1978] used the same technique to calculate celerity spectra in a series of experiments on barred beaches. He also found the measured celerity spectra constant above the peak of the energy density spectrum, but the wave celerity was anomalously low at frequencies below the peak of the spectrum. The reason for the anomalously slow wave speeds is not known. The previous measurements of the celerity spectrum in the field, although limited to a few measurement locations within the surf zone, indicate the waves might be frequency nondispersive, particularly in the shallow depth, nonlinear environment of the surf zone.

The discrepancy between linear theory and constant measured celerities has stimulated a number of papers to explain the differences. The various explanations offered, besides measurement error and measurement bias described later include: directional wave spreading [*Huang and Tung*, 1977], nonlinear coupling [*Crawford et al.*, 1981], surface drift currents [*Plant and Wright*, 1979], and changes in celerity when shorter waves ride on longer waves [*Phillips*, 1981]. All offer plausible explanations and individually or collectively could explain the observed differences.

For a linear wave system, all wave components travel at their own speed as prescribed by the linear theory dispersion relationship for phase speed

$$C = \left(\frac{g}{k}\tanh kh\right)^{1/2} \tag{10}$$

For weakly nonlinear steady uniform wave trains (e.g., Stokes waves), all the harmonics travel at the speed of the fundamental frequency (i.e., the celerity spectrum is constant). In general, a system of finite amplitude waves is composed of both free waves and forced (bound) waves. The behavior of the system will depend on the relative importance of each type of wave.

Crawford et al. [1981] investigated the relative importance of nonlinearities for one-dimensional deep water wave trains, precluding directional spreading and wave drift effects. First they showed that for a weakly nonlinear, modulated wave train all higher harmonics are nonlinearly coupled to the fundamental, no matter how small the wave steepness. The modulated wave train was simulated by a primary frequency with a symmetrical pair of lower strength side bands. Their theory predicts the amplitude of various secondary forced components at the sum and difference frequencies between the fundamental and side bands. Good comparisons were found with laboratory measurements. A modulated wave train would be similar to a very narrow band swell.

Crawford et al. [1981] next used the same theory to examine broad banded spectra which includes both forced and free waves. They found that the nonlinearity of the one-dimensional waves could explain the measured celerity spectrum discrepancies with linear theory even for small

wave slopes ($k_0a_0 \sim 10^{-2}$). The results were interpreted to indicate that nonlinearity is a possible candidate for explaining the measured celerity properties.

On the other hand, *Huang and Tung* [1977] showed that some of the discrepancies between measured celerity and linear theory could be explained by broad directional spreading of the waves. Numerical results indicated that the nonlinear influence decreases as the directional spreading of the wave energy increases. They found general agreement with a wind-wave laboratory experiment. But the observed phase speeds at higher frequencies measured in the field exceeded their computed values, indicating that directional spreading by itself is not the answer.

Phillips [1981] considered the effects of a dominant low frequency (N) wave on the celerity of higher frequency (f) waves, where the time scales were sufficiently separated ($f/N > 3$ in deep water) to use an asymptotic analysis. He found a number of long wave effects; the most important here are variations in the intrinsic short wave frequency due to distortion of the short waves riding on the long waves, and frequency Doppler shifting due to convection of the short waves by the orbital velocity of the long wave. He makes the argument that these effects are concentrated at the long wave crests so that the averaged apparent short wave speed in the direction of long wave propagation is increased by the long wave orbital velocity at the crest.

In the case of shoaling waves approaching breaking, the slope of the dominant wave train increases as do its harmonics, which propagate at the dominant wave speed. It would appear that for this case it is the dominance of these bound waves, in possible conjunction with the other effects of wave spreading and modulations of the local wave frequencies due to Doppler shifting produced by the dominant wave orbital velocities, that explain the observed differences of celerity with linear theory.

In the present experiments, we are able to examine the wave celerity spectra over a much wider range of incident conditions and at relatively closer spacings, starting well outside the surf zone and continuing across the surf zone, than in previous surf-zone studies. The data from the shallower sensors are similar to some of the above results in that the constant celerity spectra are observed suggesting frequency nondispersiveness, but frequency dispersion is clearly present in the deepest measurements. The results also suggest amplitude dispersion for measurements shallower than ~5 m. Directional spreading is considered unimportant in the present work because the measured waves were generally directionally narrow banded. Celerity spectra measurements are described first, followed by a discussion of measurement errors. Finally, a comparison is made of the mean measured celerity with shallow water wave theory.

Celerity Spectra

Celerity spectra were measured by using pairs of wave gauges or current meters separated in a line perpendicular to the beach. Consider a spectral wave component propagating toward shore and choosing for convenience the measurement points $(x_1, y_1) = (0, 0)$ and a shoreward location on a line perpendicular to the beach at $(x_2, y_2) = (\Delta x, 0)$, given by

$$\eta_1(\omega) = a_1(\omega) \cos \omega t$$
$$\eta_2(\omega) = a_2(\omega) \cos (k_x \Delta x - \omega t) \tag{11}$$

where $k_x \simeq k \cos \bar{\theta}$, is the x component of wave number $\mathbf{k}$, and $\bar{\theta}$ is the mean angle of wave incidence at frequency ω.

The phase difference between the two measurement points is given by

$$\phi(\omega) = k_x \Delta x = \frac{\omega \Delta x}{C_x'} \tag{12}$$

where $C_x' = \omega/k_x$ is the x component of celerity which is calculated by using

$$C_x' = \frac{\omega \Delta x}{\phi(\omega)} \tag{13}$$

For small angles of wave approach ($\bar{\theta} < 10°$), $C' \simeq C_x'$, with less than 2% error. In the case of a current superposed on the waves, there is a Doppler shift in the measured celerity that should be taken into account. The lowest order x component celerity accounting for a current is given by

$$C_x = C_x' - U \tag{14}$$

where U is the mean current (over the spectral averaging time for the pair of current meters) in the on-offshore direction. The mean velocity (U) was measured at a single elevation, generally closer to the bottom than the surface. The mean current is assumed uniform over depth. The differences between the velocity compensated and uncompensated celerities were generally negligible with a maximum difference of 6%. The mean measured on-offshore current was primarily a return flow going offshore, balancing the wave-induced onshore mass transport occurring in the crest-trough region. Hence, the measured celerities were generally slightly increased by inclusion of the mean current in the calculations. The celerities presented below include the mean current effect.

It should be pointed out that using separated sensors biases the measured phase information toward the forced wave phase. The forced waves are the bound harmonics of the dominant long waves. The bound harmonics would be coherent over distances on the order of the dominant wave lengths. But for the superposed free waves present, the relative separation distance increases for increasing frequency (decreasing wave length); the coherence for the free waves decreases at higher frequencies because of the relative increasing separation distance. Therefore, the more coherent bound harmonics will tend to dominate the less coherent free waves at high frequencies for the ensemble averaged phase calculation. Separating the free and forced waves is a more difficult analysis requiring bispectrum calculations.

Spectra were calculated by ensemble averaging in the frequency domain 16, 128 second records, so that each spectrum represents 34.1 min of data. A Bohman data window [*Harris*, 1976] was applied to the time series prior to spectral analysis to minimize leakage. The analysis results in each spectral estimate having approximately 57 degrees of freedom and a spectral resolution of 0.014 Hz.

Figure 5 shows the energy density, coherence, and phase difference spectra, for two current meters on November 4, 1978. The mean breaker location was between the two current meters, which were 12 m apart. The mean breaker height was ~1 m, and the spectra relatively narrow banded. Second and third harmonics are evident in the spectra. The

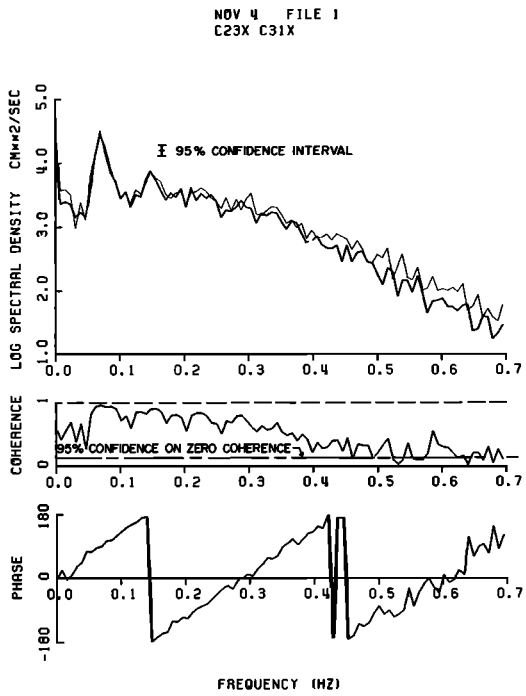

Fig. 5. Energy density, coherence and phase spectra for current meters C23 (heavy line) and C31 (light line), November 4, 1978.

coherence is high (above 0.95) in the high energy region and decreases toward higher frequencies as the energy decreases. The continuously increasing phase angle of the phase difference spectrum is indicative of progressive waves. The essentially constant slope of the phase spectrum results in a constant phase speed and is indicative of frequency nondispersive waves.

Figures 6 and 7 show measured celerity spectra (squares denote spectral estimates) at various depths proceeding from offshore (top of figure) to onshore (down the figure) for two separate days, November 12 and 20, 1978. Of 13 days analyzed, these dates are illustrated to represent a windy day (November 12) resulting in large amplitude (in 10-m depth, $H_S \sim 140$ cm) wide frequency band waves, and very narrow frequency band (Figure 8, top panel) swell type waves of moderate height (in 10-m depth $H_S \sim 80$ cm) which occurred on November 20. Up to 13 instruments along the main range line representing 12 adjacent instrument pairs were used to make the celerity calculations. Only five pairs are shown here. The sensors with a '*P*' designation are pressure sensors and '*C*' are current meters.

The solid line in Figures 6 and 7 is the celerity calculated by using the linear wave theory relationship (10). The theoretical celerities are calculated by using the mean depth between sensors, shown on each panel, and treating the bed as horizontal. The slope of the beach can be taken into account in calculating the theoretical celerity, but the corrected value is negligibly different.

The theoretical celerity predicts frequency dispersion in that the wave speed decreases with increasing frequency. The theoretical frequency dispersiveness becomes less as the depth decreases. For frequencies of about 0.3 Hz and higher, however, there is still significant theoretical frequency dispersion even at the shallowest measurement depth of 1.0 m.

The measured celerity spectra and the theoretical spectra compared well at the deepest measurements (see Figure 7) on all days except November 12 (Figure 6), demonstrating frequency dispersion. The November 12 results are used as an example because they are different and because these were the largest waves. The exception on November 12 suggests the constant celerity might be both amplitude and depth dependent.

In shallower water, there is a marked departure between measurements and linear theory for all data sets. The measured celerity becomes essentially constant with frequency as the waves approach and transect the surf zone. A horizontal line of best fit has been drawn through the calculated celerity values to indicate an average celerity. Except for offshore, the celerity spectra are essentially constant.

The range of frequencies over which the celerity spectra were calculated varied depending on several factors. The celerity spectral estimates were calculated from 0.05 to 0.5 Hz, or to the frequency at which the phase becomes unstable as measured by a deviation of more than 90 degrees between adjacent frequencies. Phase instability coincided with low coherence values, and usually occurred at a frequency corresponding to more than a two wave length separation between measurement points.

The velocity and pressure sensors were mounted less than a meter from the bottom. In the relatively deeper water at the offshore stations, the high frequency wave signals were

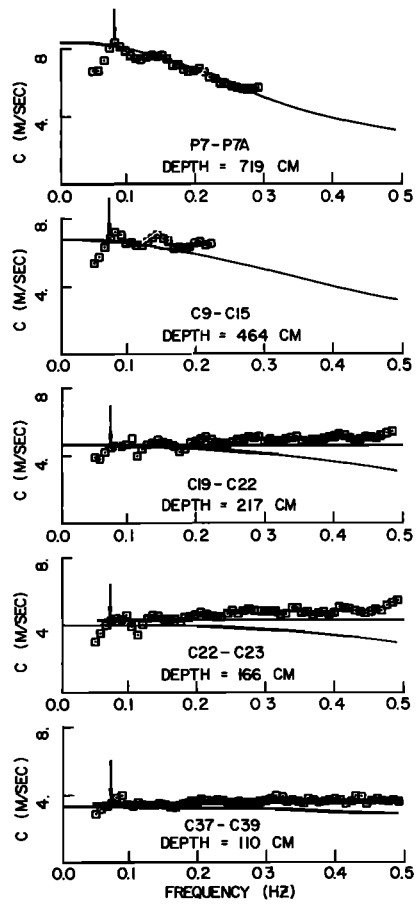

Fig. 6. Celerity spectra for relatively high waves with broad energy density spectra on November 12, 1978.

attenuated, decreasing the signal/noise ratio and coherence. As can be seen in Figure 6, the deep water celerity spectrum is truncated at about 0.3 Hz. The celerity spectra were sometimes also truncated because of phase instability at the very shallowest measurement location (see, for example, November 12). This occurs partly because wave breaking, and attendant turbulence generation, results in a decrease of signal (wave-induced velocities) to noise (turbulent velocities) ratio. The higher frequency wave signals become buried in the turbulent noise, and coherence between the two signals is decreased [*Thornton*, 1979]. Second, the wave length decreases as the depth decreases so that in very shallow water, at higher frequencies, the current meters are separated by several wave lengths. The greater the separation in wave lengths between measurement points, the less coherent the signals. As an example, the celerity spectrum on November 12 measured at the average depth of 101 cm is truncated at a frequency of 0.41 Hz, which for the 16.8 m separation between sensors corresponds to a 2.2 wave length separation at that particular frequency.

Directional properties of the incident wave field were measured with a five element linear array of pressure sensors in ~10 m depth. *Pawka* [1982] used maximum likelihood and other high resolution directional estimators to show that offshore islands and coastline orientation restrict the mean angles of swell wave approach to about ±15° deviation from normal incidence at 10 m depth with typically less than ±5° spread (half-power point) of wave angularity.

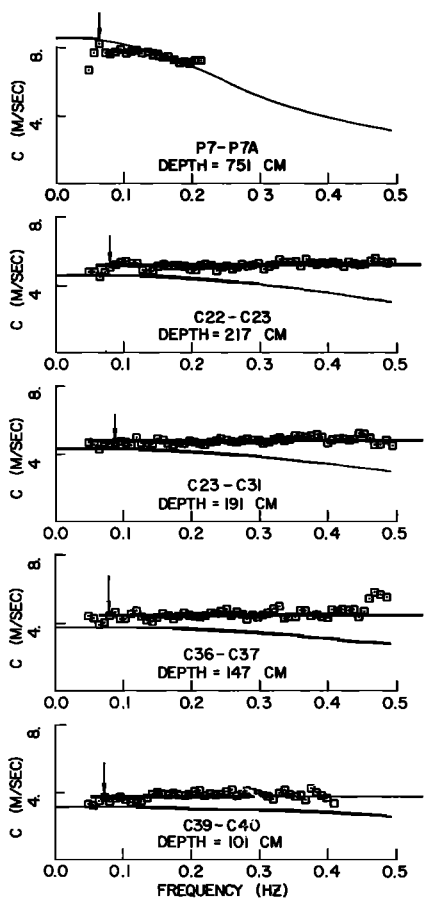

Fig. 7. Celerity spectra for moderate, very narrow-band waves on November 20, 1978.

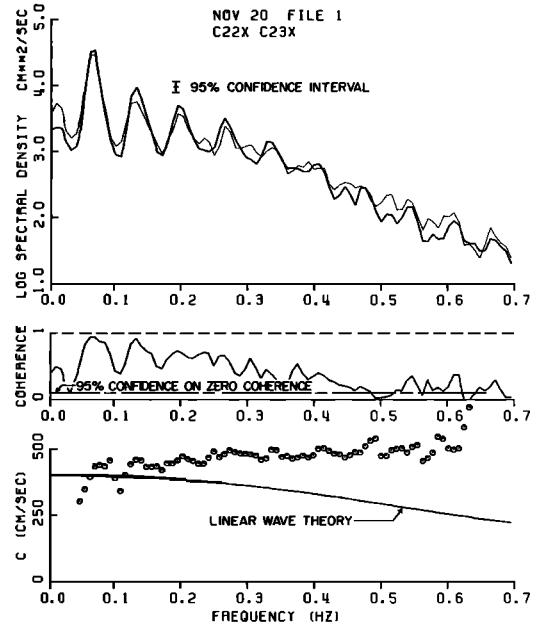

Fig. 8. Energy density, coherence and celerity spectra for current meters C22 (light line) and C23 (heavy line), November 20, 1978.

Although higher frequency waves ($f > 0.12$ Hz) can be more directionally spread because of local generation, refraction somewhat reduces local shallow water directional spreads. For example, a simple application of Snell's law to a monochromatic plane wave with a period of 13 seconds shows that refraction reduces a 15° departure from normal incidence in 10-m depth to 8.5° in 3-m and 4.9° in 1-m.

The nonlinearity of the waves in shallow water is commonly parameterized by the Ursell parameter, $Ur = a/h(kh)^2$ (with 'a' taken here as a_{rms} and k the wave number at the spectral peak). The physical region covered is from 7-m depth ($U_r \sim 0.01$) through the surf zone ($U_r \gg 1$). Thus, the waves under consideration go from weakly nonlinear to strongly nonlinear. Based on the strength of the nonlinearities and narrowness of the directional spectra, it is hypothesized the constancy of the celerity spectra is due in large part to the nonlinearity of the waves.

November 20 is an example of extreme narrow bandedness with rich harmonic growth as the waves propagate shoreward. At least five harmonics are evident in Figure 8. *Guza and Thornton* [1980] compared the ratio of energy in the first harmonic to the fundamental for this same data and found in 10-m depth a ratio of 0.08, but in 1.8-m depth (location of C22 in Figure 8) the ratio increased to 0.39. The strength of the harmonics is an indication of the nonlinearity. The waves on November 20 are a good example of a nearly one-dimensional narrow-band, modulated wave train described by *Crawford et al.* [1981] for which the celerity of the harmonics are bound to the fundamental (at least to as high a frequency as harmonics are evident or coherence is statistically significant in Figure 8).

An additional interesting phenomenon appearing in the celerity spectrum is particularly evident on days when the energy spectrum is narrow banded. As shown in Figure 8, although the waves are roughly nondispersive, there are humps and valleys in the celerity spectra which are visually correlated with the peaks and valleys of the energy density

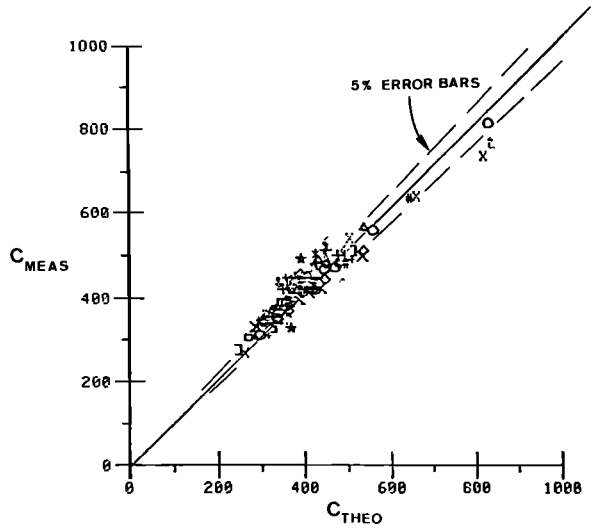

Fig. 9. Comparison of mean measured celerity with linear theory celerity.

spectra. Presumably the same nonlinear mechanisms which lead to energy peaks at the harmonics also concentrate nonlinearly induced celerity changes at these frequencies.

The constant C at higher frequencies can be attributed to the nonlinearity of the waves. It is pointed out that the constancy of celerity measurements is not a conclusive indicator of phase coupling. Bi-phase spectral calculations are required in order to be definitive; these calculations will be presented in a subsequent paper and do indicate nonlinear coupling.

Measurement Errors

The accuracy of the celerity calculations is dependent on the statistical stability of the phase estimates, and accurate measurement of the spacing between instrument locations. The comparison with theory also requires accurate depth measurement. The distances between sensors were determined by using three techniques. The offshore sensors were surveyed by using a miniranger system with an accuracy of ±1 m. The inshore stations were surveyed by tape measure and transit with accuracy of ±0.1 m. All offshore stations with wave staffs extending out of the water (C9, C15, C19) were surveyed from the beach by triangulation with a transit. In addition, a swimmer tape-measured the distance between C22 and C19 in order to close the offshore and inshore surveys. The triangulated transit distances are used since their errors are much less than a meter. Hence, the distance error is considered small.

Errors in depth cause errors in the theoretical celerity calculation. But since celerity is a function of the depth to the one-half power, the celerity calculations are relatively insensitive to errors in depth (i.e., a large fractional error in depth is required for a substantial error in celerity). The inshore depths were measured daily by using a transit level. The offshore profiles were measured three times, before, during (November 18) and after, the experiment.

Differences in comparisons with theoretical values for C occur because only the on-offshore component, C_x, was measured. Three current meters were located in a triad such that k_x could be measured using C36-C37, and k_y could be measured using C34-C36, where C34 was displaced 20-m in the alongshore direction normal to the line of C36-C37. The total celerity, C, is then calculated as

$$C = \frac{\omega}{k} = \frac{\omega}{(k_x^2 + k_y^2)^{1/2}} \tag{15}$$

Total C and C_x were calculated for comparison and the differences were not discernible when plotted on the same celerity spectrum graph. Therefore, it is concluded that C_x is generally a good estimate of C for these experiments. This is to be expected since, as mentioned above, the local angle of incident is small due to island shadowing, coastline orientation, and local refraction.

Using the distance errors above, and accounting for a nonnormal angle of wave approach, the celerity calculations at the peak of the spectrum are estimated to be accurate to within two percent inshore of C19 (approximate depth less than 3 m) and to within 5% offshore.

Mean Celerity Compared With Theory

'Mean' measured celerities are plotted in Figure 9 against linear theory celerities calculated by using the frequency at the spectral peak of the spectrum. To compare all celerity calculations, a single value was chosen to represent the spectra, which is reasonable for the constant celerity cases. Several single measures were investigated including average celerity over the spectrum, weighted average by coherence over the spectrum, celerity corresponding to the peak of the energy density spectrum, and celerity corresponding to the coherence peak. The celerity corresponding to the coherence peak (denoted in Figures 6 and 7 by an arrow over the celerity spectrum) was selected as it was easy to calculate and was found to give a consistent representative celerity for the spectrum. The frequency of the peak coherence generally coincided with the frequency at the peak of the energy density spectrum. Exceptions occurred on November 5 when the peak coherence occurred at the first harmonic of the peak of the energy density spectrum. The measured celerities are generally slightly greater than linear theory, particularly in the region of wave breaking.

Higher order, nonlinear wave theory shows that waves may be amplitude dispersive (i.e., the wave celerity is amplitude dependent). The amplitude dependence could account for some of the differences between the measured and linear theory celerities. For example, second order cnoidal wave theory celerity is given by

$$C = \sqrt{gh\left(1 + \frac{H}{h} f(E)\right)} \tag{16}$$

where $f(E)$ is a complicated Jacobian elliptic function. The shallow water asymptotic form of cnoidal theory is solitary wave theory for which

$$C_S = \sqrt{gh\left(1 + \frac{H}{h}\right)} \simeq \sqrt{gh}\left(1 + \frac{1}{2}\frac{H}{h}\right) \tag{17}$$

Simple bore theory shows a similar dependence on wave height. Comparing bore and shallow water linear wave theories

$$\frac{C_S - C_L}{C_L} = \frac{1}{2}\frac{H}{h} \tag{18}$$

The percent difference between measured and linear theory

celerity as a function of the rms wave height, H_{rms}, to depth ratio is shown in Figure 10. All mean measured celerity values, with the exception of 2, were within +20% and −10% of linear theory even at breaking and inside the surf zone. Recalling from the measurements that inside the surf zone, $H_{rms} \leq 0.42$ h; substituting this relationship into (18) (assuming H_{rms} is a correct parameterization) says that bore theory would predict the celerity about 20% greater than linear theory, which is the upper bound on the differences. The vertical line in Figure 10 is the saturation envelope relationship (6) which forms an upper bound on the abscissa. Although there is considerable scatter, there does appear to be a definite increase in difference with increasing H_{rms}/h. The dependence of celerity on wave height is indicative of amplitude dispersion.

We also note that the presence of energetic low frequency surf beat in the inner surf zone could influence wind wave phase speeds in a way analogous to the effect of wind waves on capillary waves [*Phillips*, 1981]. Surf beat rms orbital velocities are typically 0(20%) of the wind wave phase speeds in the inner surf zone. Perhaps equally important, surf beat heights are a very significant fraction of the total depth so that the mean depth over time scales of several wind wave periods will vary significantly about a longer term mean. Effects of surf beat orbital velocities and mean depth changes would both have to be considered in a theoretical study of inner surf zone phase speeds.

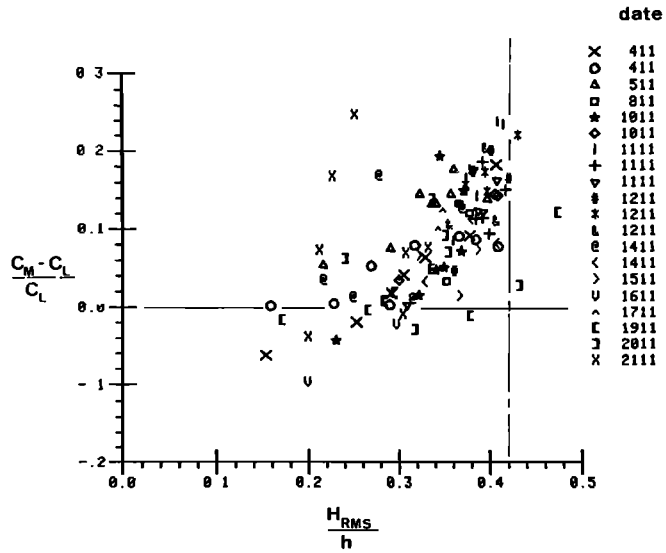

Fig. 10. Differences of measured celerity from linear wave theory as a function of wave height suggesting weak amplitude dispersion.

Conclusions

The measured transformation of the wave properties of phase speed and wave height, from 7 m shoreward are described. Only energy in the wind-wave band of frequencies is considered with the low-frequencies (<0.05 Hz) being filtered out. A primary difference between these and past experiments is the relatively close spacing of measurement locations compared to the dominant wave length along a transect on a relatively simple, almost plane beach profile.

As the waves progress across the surf zone they become locally controlled. The wind waves in the inner surf zone were strongly depth dependent with the envelope showing a linear dependence of the spilling breaker rms wave heights with depth, $H_{rms} \simeq 0.42$ h. The measured proportionality factor is considerably less than a value of 0.78 predicted by solitary wave theory which is currently incorporated in a number of dynamical models of the surf zone. The depth dependence of the spilling type breaking wave height in the inner surf zone is shown to be related to the kinematic instability criterion for breaking waves.

The celerity, or phase speed, was measured using the phase spectrum calculated between adjacent measurement locations. Celerity spectra were compared with linear wave theory. At the 7-m depth, the phase speed generally decreased with increasing wave frequency, as predicted by linear theory. As the waves progressed inshore, the celerity was found constant over the energetic region of the spectrum, even at higher frequencies where linear theory indicated the celerity should decrease. The constant celerity with increasing frequency can be an indicator of nonlinearity due to nonlinear cross spectral phase coupling dominating the free wave contribution to the averaged spectral celerity (phase) measurements. It is suggested that this was the case on at least the very narrow-band day of November 20 when the harmonics in the spectra were particularly evident.

The mean celerity, as determined from the celerity at the peak coherence, was within +20% and −10% of linear theory. The percent difference between measured celerity and linear theory was plotted against the ratio H_{rms}/h; the percent difference showed a general increase with increasing wave height to depth ratio indicating weak amplitude dispersiveness. In conclusion, the measured celerities show the waves inside 4-m are weakly amplitude dispersive, and possibly frequency nondispersive (even for high frequencies which are not, in a linear context, shallow water waves).

The increasing importance of nonlinearities on phase speeds (and hence wave number) in shallow water has implications for directional wave climate measurement programs. Many directional measurement systems (for example linear arrays and 'slope arrays' [*Higgins et al.*, 1981]) rely on the linear dispersion relation in very critical ways. For logistical reasons, these systems are frequently deployed in shallow water. The observed breakdown of the linear dispersion relation in shallow water demonstrates that inaccurate results will follow from directional measurements in 'too shallow' water. How shallow is 'too shallow' obviously depends on the wave height: 8 m depth might be 'too shallow' on November 12 (Figure 6) but may not on the rest of our data days. Perhaps it is an obvious truism that inaccurate deep water incident wave directional properties will be inferred by using linear refraction theory on a measured non-linear shallow-water wave field. Nevertheless, it is a fact seemingly ignored in many discussions of wave directional measuring systems.

Acknowledgments. This work was supported by the Office of Naval Research, Coastal Sciences Branch, under contract numbers NR 388-114 (E. B. Thornton) and N00014-75-C-0300 (R. T. Guza) and the Sea Grant Nearshore Sediment Transport Study (Project number R/CZ-N-4D). The first author wrote much of the manuscript while a Visiting Professor at the Technische Universität Braunschweig, partly supported by a Minna-James-Heineman Stiftung. R. J. Seymour obtained the bathymetric data. The encouragement of D. L. Inman is gratefully acknowledged. The staff of the shore Processes Laboratory, S.I.O., installed and maintained the offshore

sensors and data acquisition system. K. O. McCoy aided substantially in the data collection. D. O. Burych performed much of the data processing.

REFERENCES

Banner, M. L., and O. M. Phillips, On the incipient breaking of small-scale waves, *J. Fluid Mech., 4,* 646–656, 1974.

Bowen, A. J., The generation of longshore currents on a plane beach, *J. Mar. Res., 37,* 206–215, 1969.

Büsching, F., Anomalous dispersion of Fourier components of surface gravity waves in the nearshore area, in *Proceedings of the 16th International Conference Coastal Engineering,* pp. 247–267, American Society of Civil Engineers, New York, 1978.

Crawford, D. R., B. M. Lake, P. G. Saffman, and H. C. Yuen, Effects of nonlinearity and spectral bandwidth on the dispersion relation and component phase speeds of surface gravity waves, *J. Fluid Mech., 112,* 1–32, 1981.

Cunningham, P. M., R. T. Guza, and R. L. Lowe, Dynamics calibration of electromagnetic flow meters, *IEEE Oceans, 79,* 298–301, 1979.

Flick, R. E., R. L. Lowe, M. H. Freilich, and J. C. Boylls, Coastal and laboratory wavestaff system, *IEEE, Oceans '79,* 623, 1979.

Galvin, C. J., Jr., and P. S. Eagleson, Experimental study of longshore currents on a plane beach, *Tech. Memo. 10,* U.S. Army Coastal Eng. Res. Center, Fort Belvoir, Va., 1965.

Goda, Y., A Synthesis of breaker indices, *J. Civil Eng., Japan Soc. Civil Eng.,* 1970.

Guza, R. T., and E. B. Thornton, Local and shoaled comparisons of sea surface elevations, pressures and velocities, *J. Geophys. Res., 85,* 1524–1530, 1980.

Harris, F. J., Windows, harmonic analysis, and the discrete Fourier transform, *Rep. NUC TP532,* Naval Undersea Center, San Diego, Calif., 1969.

Hedges, T. S., and M. S. Kirkgöz, An experimental study of the transformation zone of plunging breakers, *Coastal Eng., 4,* 319–333, 1981.

Higgins, A. L., R. J. Seymour, and S. S. Pawka, A compact representation of ocean wave directionality, *Appl. Ocean Res., 3,* 105–112, 1981.

Huang, N. E., and C. C. Tung, The influence of the directional energy distribution on the nonlinear dispersion relation in a random gravity wave field, *J. Phys. Oceanogr., 7,* 403–414, 1977.

Inman, D. L., R. J. Tait, and C. E. Nordstrom, Mixing in the surf zone, *J. Geophys. Res., 76,* 3493–3514, 1971.

Iversen, H. W., Laboratory Study of Breakers, in Gravity Waves, *Circ. 52,* U.S. Bureau of Standards, Wash., D. C., 1952.

Longuet-Higgins, M. S., Longshore currents generated by obliquely incident sea wave, 1, *J. Geophys. Res., 75,* 6778–6789, 1970.

Longuet-Higgins, M. S., On the distribution of the heights of sea waves: Some effects of nonlinearity and finite bandwidth, *J. Geophys. Res., 85,* 1519–1523, 1980.

McCowan, J., On the solitary wave, *Philos. Mag., J. Sci., 32,* 45–58, 1891.

Miche, R., Mouvements ondulatoires des mers en profondeur constante ou decroissante, Univ. Calif. at Berkeley, Wave Res. Lab., *Ser. 3,* Issue 363, 1954.

Miller, R. L., Role of vortices in surf zone prediction: Sedimentation and wave forces, beach and nearshore sedimentation, *Spec. Publ. 24,* pp. 92–114, Society of Economic Paleontol. and Minerals, Washington D.C., 1976.

Mitsuyasu, H., Y. Kuo, and A. Masuda, On the dispersion relation of random gravity waves, 2, An experiment, *J. Fluid Mech., 92,* 731–749, 1979.

Pawka, S., Wave directional characteristics on a partially sheltered coast, Ph.D. Thesis, *Univ. of Calif., San Diego,* 1982.

Phillips, O. M., The dispersion of short wavelets in the presence of a dominant long wave, *J. Fluid Mech., 107,* 465–485, 1981.

Plant, W. J., and J. W. Wright, Spectral decomposition of short gravity wave systems, *J. Phys. Oceanogr., 9,* 621–624, 1979.

Ramamonjiarisoa, A., A. S. Baldy, and I. Choi, Laboratory studies on wind-wave generation, amplification and evolution, in *Turbulence Fluxes Through the Sea Surface, Wave Dynamics and Prediction,* edited by A. Favre and K. Hasselmann, Plenum, New York, 1978.

Stive, M. J. F., Velocity and pressure field of spilling breakers, in *Proceedings 17th International Conference on Coastal Engineering,* pp. 547–566, American Society of Civil Engineers, New York, 1980.

Suhayda, I. N., and N. R. Pettigrew, Observations of wave height and wave celerity in the surf zone, *J. Geophys. Res., 82,* 1419–1424, 1977.

Svendsen, I. A., P. A. Madsen, and J. Buhr Hansen, Wave characteristics in the surf zone, in *Proceedings 16th Coastal Engineering Conference,* pp. 520–539, American Society of Civil Engineers, New York, 1978.

Thornton, E. B., Variations of longshore current across the surf zone, in *Proceedings 12th Conference Coastal Engineering,* pp. 291–308, American Society of Civil Engineers, New York, 1971.

Thornton, E. B., Energetics of breaking waves within the surf zone, *J. Geophys. Res., 84,* 4931–4938, 1979.

Thornton, E. B., J. S. Galvin, F. L. Bub, and D. P. Richardson, Kinematics of breaking waves, in *Proceedings of 15th International Conference on Coastal Engineering,* pp. 461–476, American Society of Civil Engineers, New York, 1976.

Thornton, E. B., and R. T. Guza, Transformation of wave height distribution, submitted to *J. Geophys. Res.,* 1982.

Van Dorn, W. G., Set-up and run-up in shoaling breakers, in *Proceedings 15th International Conference Coastal Engineering,* pp. 738–751, American Society of Civil Engineers, New York, 1976.

Weggel, J. R., Maximum breaker height for design, in *Proceedings 13th International Conference Coastal Engineering,* pp. 419–432, American Society of Civil Engineers, New York, 1972.

(Received October 9, 1981;
revised July 20, 1982;
accepted July 20, 1982.)